Hexavalent Chromium Adsorption on Magnetic Nanoparticles Synthesized from Tay Nguyen Red Mud from Vietnam

Pham Thi Mai Huong[1,*], Truong Anh Thu[1], Chu Qui Thuong[1], Tran Hong Con[2] and Nguyen Thi Huong[3,*]

[1]Hanoi University of Industry, 298 Cau Dien, Bac Tu Liem, Hanoi, Vietnam
[2]VNU University of Science, 19 Le Thanh Tong, Hoan Kiem, Hanoi, Vietnam
[3]Institute of Chemistry and Materials, 17 Hoang Sam, Cau Giay, Hanoi, Vietnam

*Corresponding author: E-mail: phamthimaihuong76@yahoo.com.vn; nguyenhuong0916@gmail.com

Tay Nguyen red mud abundantly found in Vietnam, is a waste product of alumina production formed during processing of bauxite. It is rich in aluminate, residual alkaline, and oxides, such as silicon, iron, and titanium oxides. Iron oxide, which constitutes 45-55 % of Tay Nguyen, is useful for Fe_3O_4 nanoparticles synthesis. In this study, a Fe_3O_4 nanoparticles were synthesized using Tay Nguyen by the chemical co-precipitation method, which required a non-oxidizing oxygen-free environment. Fe_3O_4 nanoparticles were characterized using X-ray diffraction, field emission scanning electron microscopy, Brunauer-Emmett-Teller analysis, and vibrating-sample magnetometry. Adsorption of hexavalent chromium by the nanocomposite was conducted under batch conditions. Pseudo-second-order equations were used to describe kinetic data of adsorption reactions; the equations were fitted to kinetic data as shown by the results. The isotherms of adsorption were also studied using the linear forms of the Langmuir and Freundlich equations. The Langmuir equation exhibited higher linear correlation with the experimental data than the Freundlich equation did. The maximum monolayer coverage, q_{max} at 297 K was 31.44 mg/g.

Keywords: Tay Nguyen red mud, Hexavalent chromium, Fe_3O_4 nanoparticles, Adsorption.

INTRODUCTION

Hexavalent chromium is a typical heavy metal that features among the 25 most hazardous substances in the priority list of hazardous substances. Chromium(VI), which is present in the contaminated wastewaters is present in large volumes and high concentrations in effluents from leather tanning, plating and electroplating units, anodizing baths and rinse waters of various industrial activities. Cr(VI) in plating wastewater has a wide range of adverse effects on plants, animals and humans [1] and its toxicity can cause failure of liver, lung and kidney as well as cause gastric damage in humans even at low concentrations [2]. Currently, many techniques, such as membrane filtration, chemical precipitation, adsorption, electrodialysis, ion exchange and biological methods are used to remove Cr(VI) [3]. Among these techniques, adsorption has attracted considerable academic interests because it is an effective method in advanced wastewater treatment. The development of low-cost adsorbents

with high absorption capacities is a prominent research area in the study of materials for environmental remediation. Magnetic nanomaterials are absorption materials with a multitude of applications [4].

Some industrial waste products can be reused as low-cost absorbent material because they are produced in large volumes and are easily available. Red mud is the primary waste product of Bayer process. In Bayer process, approximately 1 to 1.5 tons of bauxite residue is generated in each cycle, for every ton of alumina produced. Furthermore, bauxite residue, an insoluble digestion by-product, is also known as red mud [5]. The use of red mud waste in different industrial processes and as raw material, such as cement clinker [6], base catalysts for biodiesel production [7] and nanostructured magnetic composites materials based on coated Fe^0 nuclei [8], has been investigated. Red mud has also been investigated as an adsorbent for inorganic compounds (phosphates and nitrates [9]) as well as arsenic [10] and heavy metals in polluted water [11].

In Vietnam, contents of Tay Nguyen red mud are as follows: iron oxide 53-54 %, Al_2O_3 15.05 % and SiO_2 5.86 % [12]; consequently, this mud has become a suitable starting point for the synthesis of Fe_3O_4 nanoparticles because of its high iron oxide content. In this study, Fe_3O_4 nanoparticles were synthesized by co-precipitation in NH_3. The adsorption isotherm, kinetic of Cr(VI) ion onto Fe_3O_4 nanoparticles produced from Tay Nguyen red mud were studied.

EXPERIMENTAL

Red mud sample was obtained from Tan Rai aluminum production plant (Tay Nguyen, Vietnam). The solution Cr(VI) (1000 mg/L), ferrous chloride tetrahydrate, sodium hydroxide and ethanol were of analytical grade and obtained from Merck (Germany). The aqueous solution was prepared with deionized water.

Synthesis of Fe_3O_4 nanoparticle from Tay Nguyen red mud: The alkaline red mud was suspended in distilled water with a liquid to solid ratio of 5:1 on a weight basis, stirring it until the equilibrium pH is 7.5 - 8.0 and dried at 80 ℃ during 24 h. The product obtained was about 50 % of iron oxide which is further treated with H_2SO_4 2 M for 3 day at room temparature. Then the mixture was liltered to remove insoluble solids and a red mud solution was obtained.

$FeCl_2·4H_2O$ (with 1:2 molar ratio) were simultaneously added in a deoxygenated 100 mL red mud solution with vigorous stirring under N_2 gas flow. The reaction mixture is stirred for 10 min, while aerating nitrogen to obtain a yellow-orange solution. Slowly added 25-28 % NH_3 solution to the reaction flask so that the solution always maintains pH 9-10. At this time, the solution turns from yellow-orange to brown then black. After adding sufficient NH_3, continue the reaction for 1 h, maintaining the reaction conditions. The product was a black precipitate, then it is separated by a magnet and washed with deionized water and ethanol, and finally dried at 70 ℃ for 12 h in a vacuum oven (signed as RMN2).

Characterization of Fe_3O_4 nanoparticle: The crystalline formation of the magnetite in RMN2 was studied by X-ray diffraction (XRD). The morphology of magnetite Fe_3O_4 nanoparticle was investigated by scanning electron microscopy (SEM), specific area was measured by BET adsorption and elemental composition was observed by energy dispersive X-ray spectroscopy (EDX), magnetic measurements of solid samples were performed at room temperature (25 ℃) using a Magnet B-10 Vibrating sample magnetometer (VSM).

Adsorption of Cr(VI) by Fe_3O_4 nanoparticles: Bath adsorption mode with Cr(VI) solution of 15 mg/L and the ratio of solid (Fe_3O_4 nanomaterial) and liquid (Cr(VI) solution)-phases were 1 g/100 mL. The initial pHs of adsorption solution was adjusted for each experiment by HCl or NaOH solution (0.1 M). The adsorption mixtures were mixed around on shaker at 180 rpm for designed contact time and in constant of room temperature. After contacted times, solid phase was separated by filtration through paper membrane with 0.45 µm porosity. The remained of Cr(VI) concentration in the aqueous solution were determined by using a Thermo Scientific GENESYS Ultraviolet-visible spectrophotometer analyser at λ = 540 nm using 1,5-diphenylcarbazide method [13].

Adsorption capacity of Fe_3O_4 nanoparticle is calculated by the following equation [14]:

$$q = \frac{(C_o - C_t)·V}{m} \tag{1}$$

where, V is the volume of solution (L); m is the mass of adsorbent (g); C_o and C_t are Cr (VI) concentrations in the initial solution and at time t, respectively (mg/L). The Langmuir and Freundlich isothermal models were applied for discussion of adsorption characterization and properties of adsorption processes.

RESULTS AND DISCUSSION

XRD analysis: XRD was recorded on a D8-Advance, Bruker and Siemen D5005, X-Ray diffractometer using Cu $K\alpha$ (λ = 1.5406 Å) at 40 kV. The XRD spectrum of RMN2 (Fig. 1) shows the presence of magnetite (Fe_3O_4) crystal at peaks 280º, 350º and 270º. The position and relative intensity of all peaks match well with standard Fe_3O_4 powder diffraction data [10]
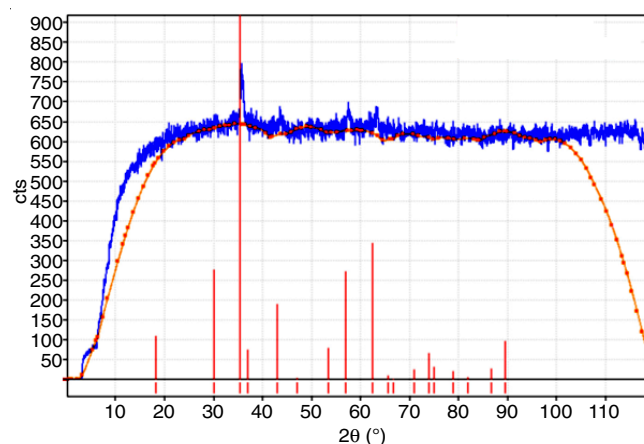

Fig. 1. XRD spectra of magnetite Fe_3O_4 nanoparticle (RMN2)

The obtained black precipitate, which can be attracted by a permanent magnet proved the formation of Fe_3O_4 crystals. SEM image and nitrogen adsorption-desorption isotherms and Barrett-Joyner-Halenda (BJH) pore-size distribution for Fe_3O_4 nanoparticle at 77 K have been shown in Figs. 2 and 3, respectively. The mean diameter of Fe_3O_4 nanoparticle particles were determined to be 10-20 nm.
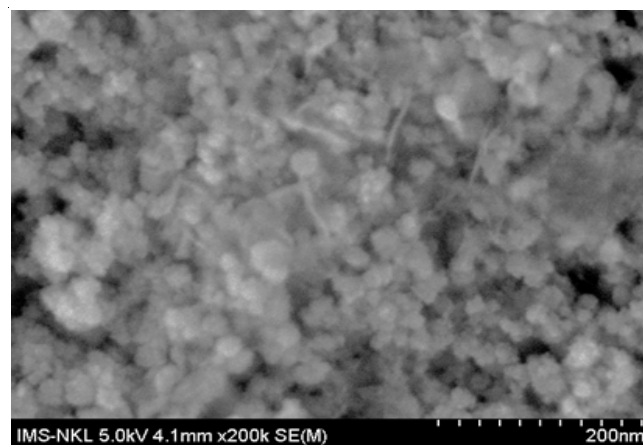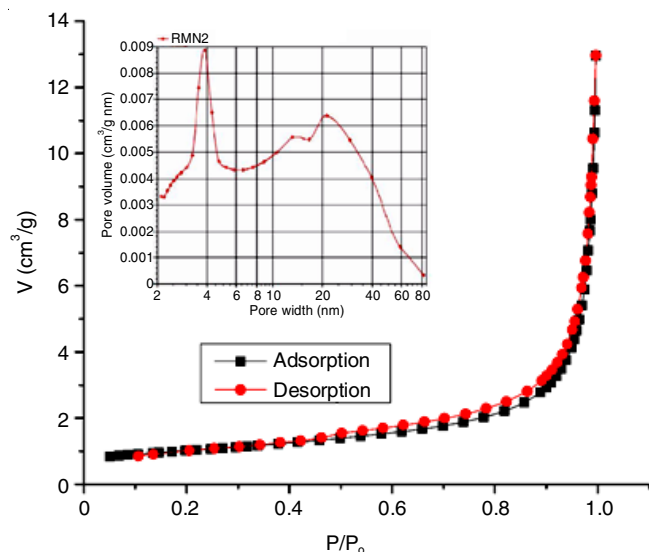

Fig. 2. SEM images of RMN2

Fig. 3. Nitrogen adsorption–desorption isotherms and Barrett-Joyner-Halenda (BJH) pore-size distribution for Fe_3O_4 nanocomposite at 77 K

From Fig. 3, it is shown that Fe_3O_4 nanocomposite samples give adsorption-desorption, Fe_3O_4 nanoparticle samples give adsorption-desorption isotherm of type IV and H3 hysteresis loop, rod-shaped and letter shaped according to IUPAC classification [15]. This allows the prediction that synthetic nanoparticle materials contain both mesopore and macropore, in which the mesoporous are abundant. The measured BET surface areas of Fe_3O_4 nanoparticle was found to be 60.64 m^2/g. The total pore volume of Fe_3O_4 nanoparticle was 0.2407 cm^3 g^{-1} and the average of pore size distribution for Fe_3O_4 nanoparticle was 15.38 nm. Similarly, the saturation magnetization was found to be 36 emu/g (Fig. 4), which means that synthesized Fe_3O_4 nanoparticles (RMN2) could be easily attracted using a conventional magnet.

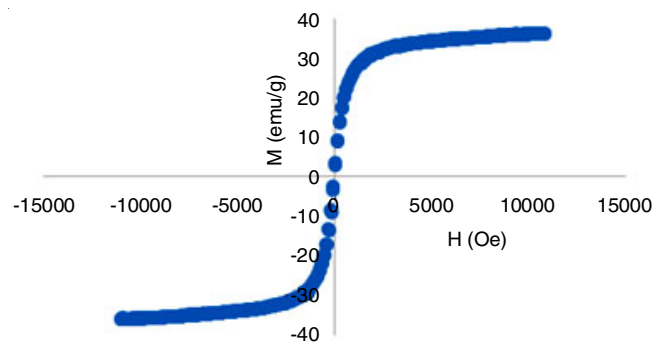
Fig. 4. Magnetization curves of magnetite particles at room temperature (297 K)

Study of Cr(VI) adsorption by the synthesized material

Effect of pH on adsorption ability: One of the most influential factors on Cr(VI) removal is the pH of the solution, which influences on the properties of adsorption and self adsorption. In this experiment, the initial concentration of Cr(VI) was 15 mg/L and the initial pH values of adsorption solution were adjusted in the range of 2 to 10 and the contact time was 90 min. The amount of Cr(VI) adsorbed depends on the distribution of $Cr_2O_7^{2-}$, $HCrO_4^-$ and CrO_4^{2-} which are controlled by

pH of the solution. In acidic medium, Cr(VI) exists in the form of oxyanions such as $Cr_2O_7^{2-}$, $HCrO_4^-$ and CrO_4^{2-}. The lowering of pH causes the surface of adsorbent to be protonated to a higher extent, a strong attraction exists between these oxyanions of Cr(VI) and the positively charged surface of the adsorbent. Hence, the uptake increases with increasing pH from 4.0 to 2.0 of solution. Whereas at high pH, there will be abundance of negatively charged hydroxyl ions in aqueous solution, causing hindrance between negatively charged ions $Cr_2O_7^{2-}$, $HCrO_4^-$, CrO_4^{2-} and negatively charged adsorbent, resulting in a decrease of adsorption. However, the survey process was carried out from pH = 4 to pH = 10 because, at points of pH less than 4, the dissolution of Fe_3O_4 nanoparticles occurs [16].

At higher pH values, the adsorption efficiency of Cr(VI) decreased due to competition of OH^- anion and loss of electropositive effect of Fe_3O_4 nanoparticle surfaces.

Effect of contact time and kinetic evaluation: The effect of contact time on chromium(VI) adsorption was investigated to determine equilibrium time for the adsorption process. The initial Cr(VI) concentration was 15 mg/L having pH 6.0. The results are shown in Fig. 5. It could be seen that the optimum time is 90 min to get adsorption equilibrium for Cr(VI) on the Fe_3O_4 nanoparticles.
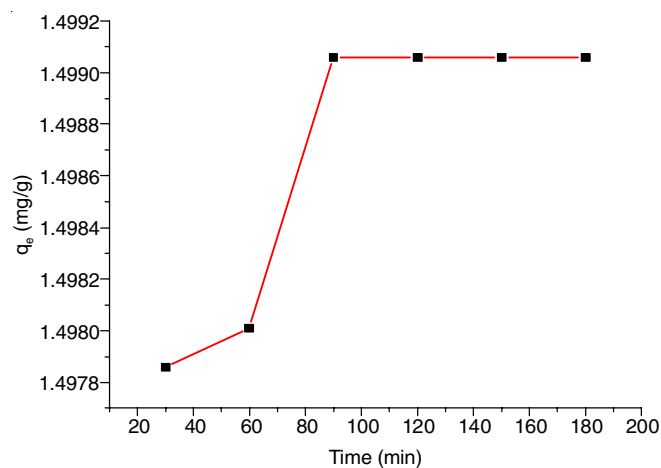

Fig. 5. Effect of contact time on the sorption of Cr(VI) by Fe_3O_4 nanoparticle material

In order to study the adsorption kinetics, a linear form of pseudo-second order adsorption is applied, which is given as:

$$\frac{t}{q_t} = \frac{t}{q_e} + \frac{1}{k_2 \cdot q_e^2} \qquad (2)$$

where q_e, q_t are the adsorption capacities at equilibrium time and time t, k_2 (mg/g min) is the rate constant of adsorption kinetics process [17,18].

Other adsorption models such as diffusion kinetics [19] and Elovich equation [20] were also considered as they are useful for the prediction of the adsorbent-adsorbate interaction.

Diffusion kinetics:

$$\ln(q_t) = \ln(k_D) + 0.5 \cdot \ln(t) \qquad (3)$$

where k_D (mg/g $min^{0.5}$) is the diffusion coefficient.

Elovich equation:

$$q_t = \frac{1}{\beta} \ln(\alpha\beta) + \frac{1}{\beta} \ln(t) \qquad (4)$$

	TABLE-1						
	KINETIC PARAMETERS FOR THE REMOVAL OF Cr(VI) ONTO RMN2						
C_o (ppm)	Pseudo second order		Intraparticle diffusion		Elovich model		
	R^2	k_2	R^2	K_D	R^2	α	β
15	1.0000	24.31087	0.9705	1.49525	0.9704	-0.1499	0.000794

where α and β are constants of Elovich equation.

The linear regression equations of t/q_t on t for second-order kinetic model, $\ln q_e$ on $\ln t$ for diffusion kinetics model and q_t on $\ln t$ for Elovich model are shown in Fig. 6. From the value of the slopes and the intercepts of straight line equations, it is possible to calculate the respective kinetic equation constants and the data is shown in Table-1.

From the results in Table-1, it is shown that the pseudo-second-order adsorption kinetics equation has a correlation coefficient of approximately 1, which indicates that the speed constant does not depend on concentration. This proves that the adsorption process depends on the number of adsorption centers on the surface and the adsorbate.

Adsorption isotherms of Cr(VI): The experimental data was analyzed with well-known adsorption isotherm models *viz.* the Langmuir and Freundlich isotherms. All adsorption and desorption experiments were carried out at room temperature (297 ± 1 K). The initial Cr (VI) concentrations was ranged from 1 to 200 mg/L. The experiments were caried out using 100 mL of Cr (VI) solution at pH 6.0, the contact time was 90 min and the adsorbent dose was 1 g L^{-1}. All the experimental data were the average of triplicate determinations.

The linear equations of Langmuir and Freundlich isotherm models can be described as follows [21]:

$$\frac{C_e}{q_e} = \frac{1}{Q_o b} + \frac{C_e}{q_e} \qquad (5)$$

where C_e is the concentration of Cr(VI) ion (mg/L) at equilibrium, Q_o is the monolayer capacity of the adsorbent (mg/g) and b is the Langmuir sorption constant (L/mg). The plot of C_e/q_e *versus* C_e gives a straight line and the values of Q_o and b can be calculated from the slope and intercept of the plot.

$$\log q_e = \log K + \frac{1}{n} \log C_e \qquad (6)$$

where C_e is the equilibrium concentration (mg/L), k is a roughly indicator of the adsorption capacity and n is an empirical parameter. The plot of $\log q_e$ *versus* $\log C_e$ gives a straight line

and k and n values are calculated from the intercept and slope of this straight line.

The related values of parameters and constants for these isotherms are presented in Table-2. As the results show, the obtained data better fitted to a Langmuir isotherm ($R^2 = 0.9779$) compared to the Frendlich isotherm.

TABLE-2					
PARAMETER OF LANGMUIR AND FRENDLICH ISOTHERMS FOR ADSORPTION OF Cr(VI) ON THE RMN2					
Langmuir isotherm model			Freundlich isotherm model		
q_{max} (mg/g)	K_L	R^2	n	K_F	R^2
31.44	1.0394	0.9779	1.3099	1.1790	0.9023

The adsorption capacity of Fe_3O_4 nanoparticle Cr(VI) is compared with other reported adsorbents and summarized in Table-3. Thus, from Table-3, one can predict easily that synthesized magnetic nanoparticles from Tay Nguyen red mud is highly adsorptive for chromium(VI) ions.

TABLE-3		
COMPARISON OF ADSORPTION CAPACITY OF Fe_3O_4 NANOCOMPOSITE FOR Cr(VI) WITH PREVIOUSLY REPORTED ADSORBENTS		
Adsorbents	Adsorption capacity (mg g^{-1})	Ref.
Red mud	4.36	[22]
Carbon slurry	15.24	[23]
Talc powder	26.59	[21]
Cetyltrimethylammonium bromide/red mud	22.20	[24]
Fe_3O_4 nanocomposite	31.44	Present study

Conclusion

In this work, magnetic nanoparticles synthesized from Tay Nguyen red mud were used as absorbents for the removal of chromium(VI) ions. The surface area of synthesized nanoparticles was determined to be 60.64 m^2/g using the BET method.
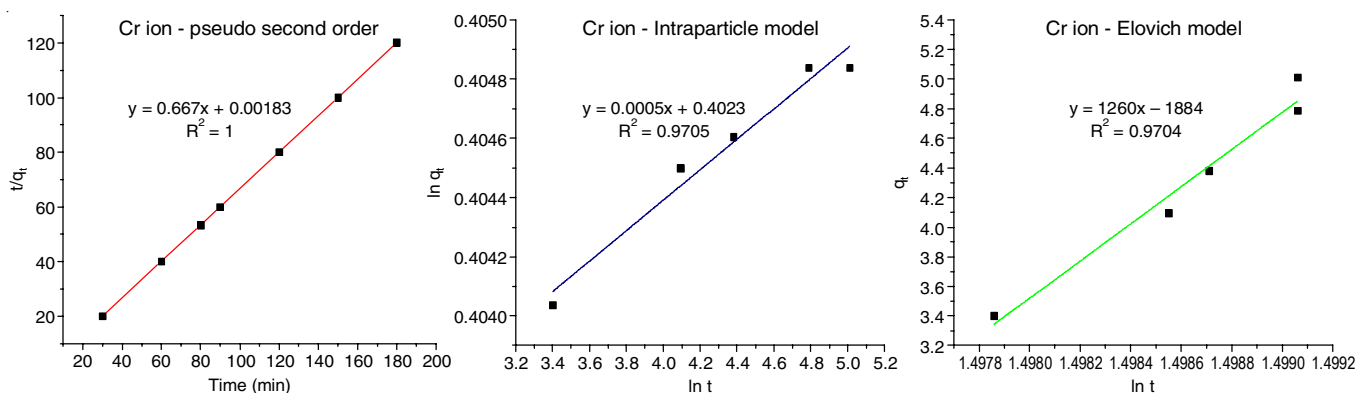

Fig. 6. Kinetic models of adsorption of Cr(VI) ion on the Fe_3O_4 nanoparticle (RMN2)

The total pore volume and the average of pore size distribution for Fe_3O_4 nanoparticle were found to be 0.2407 cm^3 g^{-1} and 15.38 nm, respectively. The maximum adsorption capacity of synthesized Fe_3O_4 nanoparticle was 31.44 mg/g occurred at pH 6.0 and 297 K. These results permit to conclude that Fe_3O_4 nanoparticle is a promising low-cost adsorbent for Cr (VI) ions removal from wastewaters and can be applied in a magnetically-assisted water treatment technology.

CONFLICT OF INTEREST

The authors declare that there is no conflict of interests regarding the publication of this article.

REFERENCES

1. Z. Liu, G. Wang and X. Zhao, *J. Wuhan Univ. Technol.*, **25**, 323 (2010);
   https://doi.org/10.1007/s11595-010-2323-x
2. W. Daoud, T. Ebadi and A. Fahimifar, *Korean J. Chem. Eng.*, **32**, 1119 (2015);
   https://doi.org/10.1007/s11814-014-0337-3
3. M. Owlad, M.K. Aroua, W.A.W. Daud and S. Baroutian, *Water Air Soil Pollut.*, **200**, 59 (2009);
   https://doi.org/10.1007/s11270-008-9893-7
4. J. Gimenez, M. Martinez, J. Depablo, M. Rovira and L. Duro, *J. Hazard. Mater.*, **141**, 575 (2007);
   https://doi.org/10.1016/j.jhazmat.2006.07.020
5. S. Kumar, R. Kumar and A. Bandopadhyay, *Resour. Conserv. Recycling*, **48**, 301 (2006);
   https://doi.org/10.1016/j.resconrec.2006.03.003
6. P.E. Tsakiridis, S. Agatzini-Leonardou and P. Oustadakis, *J. Hazard. Mater.*, **116**, 103 (2004);
   https://doi.org/10.1016/j.jhazmat.2004.08.002
7. Q. Liu, R. Xin, C. Li, C. Xu and J. Yang, *J. Environ. Sci. (China)*, **25**, 823 (2013);
   https://doi.org/10.1016/S1001-0742(12)60067-9
8. A.A.S. Oliveira, J.C. Tristão, J.D. Ardisson, A. Dias and R.M. Lago, *Appl. Catal. B*, **105**, 163 (2011);
   https://doi.org/10.1016/j.apcatb.2011.04.007
9. Y. Li, C. Liu, Z. Luan, X. Peng, C. Zhu, Z. Chen, Z. Zhang, J. Fan and Z. Jia, *J. Hazard. Mater.*, **137**, 374 (2006);
   https://doi.org/10.1016/j.jhazmat.2006.02.011
10. I. Akin, G. Arslan, A. Tor, M. Ersoz and Y. Cengeloglu, *J. Hazard. Mater.*, **235-236**, 62 (2012);
    https://doi.org/10.1016/j.jhazmat.2012.06.024
11. F.T. da Conceição, B.C. Pichinelli, M.S.G. Silva, R.B. Moruzzi, A.A. Menegário and M.L.P. Antunes, *Environ. Earth Sci.*, **75**, 362 (2016);
    https://doi.org/10.1007/s12665-015-4929-y
12. P.T.M. Huong, T.H. Con and T.T. Dung, *Environ. Asia*, **10**, 86 (2017);
    https://doi.org/10.14456/ea.2017.24
13. K.K. Onchoke and S.A. Sasu, *Adv. Environ.*, **2016**, Article ID 3468635 (2016);
    https://doi.org/10.1155/2016/3468635
14. W.S.W. Ngah and S. Fatinathan, *J. Environ. Manage.*, **91**, 958 (2010);
    https://doi.org/10.1016/j.jenvman.2009.12.003
15. M. Thommes, K. Kaneko, A.V. Neimark, J.P. Olivier, F. Rodriguez-Reinoso, J. Rouquerol and K.S.W. Sing, *Pure Appl. Chem.*, **87**, 1051 (2015);
    https://doi.org/10.1515/pac-2014-1117
16. M. Iram, C. Guo, Y. Guan, A. Ishfaq and H. Liu, *J. Hazard. Mater.*, **181**, 1039 (2010);
    https://doi.org/10.1016/j.jhazmat.2010.05.119
17. H. Yuh-Shan, *Scientometrics*, **59**, 171 (2004);
    https://doi.org/10.1023/B:SCIE.0000013305.99473.cf
18. Y.S. Ho, Absorption of Heavy Metals from Waste Streams by Peat, Ph.D. Thesis, University of Birmingham, Birmingham, U.K. (1995).
19. P. Ge and F.T. Li, *Pol. J. Environ. Stud.*, **20**, 339 (2011).
20. A.S. Thajeel, *Aquatic Sci. Technol.*, **1**, (2013).
21. M.E. Ossman, M.S. Mansour, M.A. Fattah, N. Taha and Y. Kiros, *Bulg. Chem. Commun.*, **46**, 629 (2014).
22. V.K. Gupta, M. Gupta and S. Sharma, *Water Res.*, **35**, 1125 (2001);
    https://doi.org/10.1016/S0043-1354(00)00389-4
23. V.K. Gupta, A. Rastogi and A. Nayak, *J. Colloid Interface Sci.*, **342**, 135 (2010);
    https://doi.org/10.1016/j.jcis.2009.09.065
24. D. Li, Y. Ding, L. Li, Z. Chang, Z. Rao and L. Lu, *Environ. Technol.*, **36**, 1084 (2015);
    https://doi.org/10.1080/09593330.2014.975286